



Published in final edited form as:

Neuron. 2016 August 17; 91(4): 863–877. doi:10.1016/j.neuron.2016.07.013.

The Basis of Food Texture Sensation in *Drosophila*

Yali V. Zhang^{1,*}, Timothy J. Aikin¹, Zhengzheng Li², and Craig Montell^{1,*}

¹Neuroscience Research Institute and Department of Molecular, Cellular and Developmental Biology, University of California Santa Barbara, Santa Barbara, CA, 93106, USA

²Department of Biological Chemistry, The Johns Hopkins University School of Medicine Baltimore, MD 21205, USA

Summary

Food texture has enormous effects on food preferences. However, the mechanosensory cells and key molecules responsible for sensing the physical properties of food are unknown. Here, we show that akin to mammals, the fruit fly, *Drosophila melanogaster*, prefers food with a specific hardness or viscosity. This food texture discrimination depends upon a previously unknown multidendritic (md-L) neuron, which extends elaborate dendritic arbors innervating the bases of taste hairs. The md-L neurons exhibit directional selectivity in response to mechanical stimuli. Moreover, these neurons orchestrate different feeding behaviors depending on the magnitude of the stimulus. We demonstrate that the single *Drosophila* transmembrane channel-like (TMC) is expressed in md-L neurons, where it is required for sensing two key textural features of food—hardness and viscosity. We propose that md-L neurons are long-sought-after mechanoreceptor cells through which food mechanics are perceived and encoded by a taste organ, and this sensation depends on TMC.

eTOC Blurp

Zhang et al. established *Drosophila* as a model to reveal how animals evaluate food texture. They identified a multidendritic neuron in the fly tongue, and the transmembrane channel-like homolog, which are critical for selecting foods based on hardness and viscosity.

Introduction

Food preferences are affected greatly by the qualities of food, including nutrient value, texture, and the taste valence of sweet, bitter, salty and sour qualities (Foster et al., 2011; Freeman and Dahanukar, 2015; Galindo et al., 2012; Joseph and Carlson, 2015; Koc et al.,

*To whom correspondence should be addressed: craig.montell@lifesci.ucsb.edu or yali.zhang@lifesci.ucsb.edu.

Author Contributions

Y.V.Z. and C.M. conceived the project, planned the experiments, interpreted the results and wrote the manuscript. Y.V.Z. conducted most of the experiments. T.A. performed some molecular biology experiments and Z.L. generated the *tmc-QF* transgenic fly line.

Supplemental Information

The Supplemental Information includes eight figures, Supplemental Experimental Procedures and supplemental references.

Publisher's Disclaimer: This is a PDF file of an unedited manuscript that has been accepted for publication. As a service to our customers we are providing this early version of the manuscript. The manuscript will undergo copyediting, typesetting, and review of the resulting proof before it is published in its final citable form. Please note that during the production process errors may be discovered which could affect the content, and all legal disclaimers that apply to the journal pertain.

2013; Liman et al., 2014). During the last fifteen years, many of the gustatory receptor proteins that participate in the discrimination of the chemical composition of food have been defined (Liman et al., 2014). In sharp contrast, the basis through which food texture is detected is enigmatic, despite the universal appreciation that the physical properties of food greatly influence decisions to consume a prospective offering (Rolls, 2005).

There are specific tactile features associated with liquid or solid food. Viscosity and creaminess are typical textural features of liquid food, whereas hardness, crispiness, and softness are the main physical characteristics of solid food (Koc et al., 2013). Similar to food tastes, food texture provides important information concerning food quality including freshness and wholesomeness. For instance, people prefer freshly baked bread with relatively soft texture, and tend to reject older bread with a harder texture, even though their chemical composition has not changed significantly over the course of a couple of days. Furthermore, while exploring the food landscape, an animal must make assessments of food hardness and viscosity in order to exert the appropriate force to chew or ingest (Foster et al., 2011; Koc et al., 2013). Insufficient chewing force results in poor food processing, while excessive force can cause injury to the tongue or teeth.

Food texture in mammals is predominantly detected through poorly understood mechanisms in taste organs. In rodents and humans, a subset of trigeminal nerves such as the lingual nerve provides somatosensitive afferents to the tongue (Westberg and Kolta, 2011; Whitehead et al., 1985). Due to the intrinsic mechanical properties of food, mastication produces compression and shearing forces, which in turn activate mechanosensory neurons in taste organs. However, the molecular identities of mechanosensory neurons and signaling proteins that enable animals to detect food texture are unknown.

To address the fundamental issue concerning the cellular and molecular mechanisms that function in the sensation of food texture, we turned to the fruit fly, *Drosophila melanogaster*, as an animal model. In flies, food quality is evaluated largely through external sensory hairs (sensilla), which decorate the fly tongue (the labellum) and several other body parts (Liman et al., 2014). These sensilla, which house several sensory neurons, allow the chemical composition of foods, such as sugars and bitter compounds, to be detected prior to entering the mouthparts.

Here, we found that *Drosophila* can discriminate between foods on the basis of hardness and viscosity. We identify a previously unknown type of mechanosensory neuron in the fly tongue that is dedicated to detecting food mechanics. These multidendritic neurons in the labellum (md-L) extend their projections into the bases of most of the external sensilla, and are activated by deflections induced by hard and viscous food. The ability of md-L neurons to sense food mechanics is virtually lost due to elimination of the only *Drosophila* member of the transmembrane channel-like (TMC) family. Mice and humans each encode eight TMC proteins (Keresztes et al., 2003), and mutations in the founding member of this family, *TMC1*, cause deafness in mammals (Kurima et al., 2002; Vreugde et al., 2002). We found that *tmc* is broadly tuned to detect both soft and hard food textures. Remarkably, optogenetic stimulation of the md-L neurons with different light intensities yields opposing behavioral outcomes— weak light promotes feeding while strong light represses feeding. We conclude

that md-L neurons and TMC are critical cellular and molecular components that enable external sensory bristles on the fly tongue to communicate textural features to the brain, and do so through a pre-ingestive mechanism.

Results

Fruit flies prefer food with a specific hardness and viscosity

We chose the fruit fly as a potential animal model to uncover mechanisms through which basic food textures, such as viscosity for liquid food and hardness for solid food, affect taste preference (Liman et al., 2014). To explore how the viscosity of liquid food influences feeding behavior, we used a colorless, odorless and tasteless chemical, hydroxypropyl cellulose (HPC), since low levels of HPC dissolved in water (0.5—1.5%) give rise to a wide range of viscosities (Figure 1A). Moreover, using tip recordings to assay action potentials in fly gustatory receptor neurons (GRNs), we established that 0.5—1.5% of HPC did not elicit gustatory activity (Figures 1B and 1C). However, when HPC was mixed with 100 mM sucrose, it had little effect on sugar-induced action potentials (Figures 1B and 1C). Taken together, HPC is an ideal chemical compound to assess the impact of viscosity on feeding in that it causes a striking change in food viscosity without modifying intrinsic food taste.

Next, we used HPC to examine how wild-type flies respond to liquid foods of different viscosities. Towards this end, we conducted proboscis extension reflex (PER) assays. We constrained the legs and wings of the flies within a small pipet tip, which left the proboscis and head exposed (Figure 1D). We then touched the proboscis using a drop of sucrose solution (100 mM) mixed with different concentrations of HPC (0—1.5%). Pre-starved flies readily accepted sucrose solutions by extending their proboscis (Figure 1E). However, as the sucrose solution became more viscous, the animals showed a significant decline in receptivity to the liquid food (Figures 1F and 1G).

We then asked whether the hardness of solid food impacted on feeding behavior in fruit flies. To test this idea, we chose agarose as a food-gelling ingredient because food viscoelasticity could be changed readily by varying the concentration of agarose. Furthermore, since agarose is nontoxic, tasteless, and odorless, it serves as an excellent food-supporting material that allows us to investigate the sole contribution of food hardness to feeding behavior. The minimal agarose concentration that can form solid food is ~0.5%. To quantitatively characterize food texture, we performed rheological measurements (Vélez-Ruiz and Barbosa Cánovas, 1997) using 2 mM sucrose combined with a spectrum of agarose concentrations. According to our rheometric assays, the stiffness, or hardness of food increased exponentially as the agarose concentration rose (Figure 1H).

To analyze the impact of food hardness on feeding behavior, we conducted two-way choice assays using a Petri dish (Figure S1) (Zhang et al., 2013). One half of the dish contained 2 mM sucrose and 1% agarose, while the other half contained 2 mM sucrose and a series of agarose concentrations ranging from 0.5—4%. With this instrument, we subjected the control flies to two-way feeding behavioral assays, and assessed food preference by inspecting the color of their abdomens due to the food dyes. We found that flies preferred consuming food with 1% agarose over softer food (0.5% agarose) and harder foods with

decreasing preference as stiffness increases (2—4% agarose; Figure 1I). Furthermore, to ascertain that the food hardness was directly sensed through the primary taste organ, the proboscis, we performed PER assays using 0.5—4% agarose gelled with 100 mM sucrose. Consistent with the two-way feeding assays, the PER assays showed that as the agarose concentration rose from 0.5% to 1%, the wild-type flies exhibited enhanced food preferences, while the animals showed a gradual decrease in food preference as the agarose concentration increased above 1% (Figure 1J). Taken together, flies show bi-directional food preferences for foods with varying agarose concentrations, and they prefer food with 1% agarose.

Our data indicate that fruit flies elicit gustatory preferences based on viscosity and hardness. Moreover, flies discriminate these fundamental textural properties of liquid and solid foods pre-ingestively, similar to the discrimination of sugars and aversive compounds, which is sensed through GRNs in sensory sensilla external to the mouth parts (Liman et al., 2014).

Requirement for *tmc* for discriminating the hardness of food

To identify candidate molecules that contribute to the detection of a physical property of food, we screened mutants and RNAi lines disrupting a number of different classes of receptors and ion channels that are known to be expressed in the labellum or function in taste and other sensory modalities. These include gustatory receptors (GRs), ionotropic receptors (IRs) and transient receptor potential (TRP) channels, several of which are known mechanosensors involved in touch, proprioception and hearing (Akitake et al., 2015; Benton et al., 2009; Effertz et al., 2012; Koh et al., 2014; Walker et al., 2000; Yan et al., 2013). None of these candidates were required for sensing food mechanics (Figure 2A). Flies lacking the Piezo channel (Kim et al., 2012) also showed normal discrimination of food hardness (Figure 2A).

We also tested a role for *Drosophila* TMC, since mammalian TMC1 and TMC2 affect hearing (Kurima et al., 2002; Pan et al., 2013; Vreugde et al., 2002), and therefore may have sensory roles in flies. As opposed to mice and humans, each of which encodes eight TMC family members, fruit flies encode only a single TMC homolog (Kurima et al., 2003). To address whether *Drosophila tmc* was required for sensing food texture, we obtained a fly line with a transposon (PiggyBac; *tmc^{PB}*), which inserted in the DNA sequence encoding residue 1,365 of the 1,932 amino acid TMC protein. We then compared the control and *tmc^{PB}* preferences between sucrose embedded in either 1% agarose or 3% agarose. Most wild-type animals chose food containing 1% agarose. However, *tmc^{PB}* mutant animals exhibited a moderate deficit in choosing 1% agarose food (Figure 2A).

Given the mild abnormality displayed by the *tmc^{PB}* mutant, we generated a null allele (*tmc^Δ*) by homologous recombination. The 500 base pair deletion included the genomic fragment encoding the 120 amino acid TMC domain (Figure 2B; Figures S2A and S2B), which is highly conserved among human, mouse, fly and worm TMCs (>50% identity) (Kurima et al., 2003), suggesting that this region plays an evolutionally indispensable role. In addition, the deletion changed the reading frame and also deleted several donor and acceptor sites used for mRNA splicing. As a consequence, the mRNA transcript is no longer properly

processed and is therefore undetectable in *tmc¹* flies (Figure S2C). The *tmc¹* flies were viable, healthy and appeared morphologically normal.

Next, we tested the capability of null *tmc¹* flies to discriminate foods of different stiffness by varying the agarose concentration from 0.5—4%. Based on two-way choice assays, *tmc¹* flies showed severe impairments in discriminating 1% agarose-containing food from softer or harder agarose foods (Figure 2C). Moreover, wild type flies preferred slightly hard food (2% agarose) over moderately hard (3% agarose) or very hard food (4% agarose; Figures S3A—S3C). In contrast, *tmc¹* animals showed impairments in discriminating between different hard foods (Figures S3A—S3C). The deficits in avoiding hard foods exhibited by *tmc¹* were more severe than displayed by *tmc^{PB}* (Figure S3D). Strikingly, using the PER assays, *tmc¹* flies had similar preferences for sucrose-containing soft food (1% agarose) and hard food (4% agarose; Figure 2D). Consequently, the mutant flies showed a lower PER relative to controls in response to the soft food and much higher responses to hard food (Figure 2D), indicating that *tmc* is required to sense both soft and hard foods. The *tmc¹* mutant also showed severe deficits in discriminating liquid foods with different levels of viscosity (Figure 2E). The defects in discriminating food texture were not secondary to a general feeding abnormality, as *tmc¹* mutants exhibited normal avoidance of bitter tastants such as quinine, denatonium, strychnine and berberine (Figure S3E). Taken together, *tmc¹* mutant flies did not display a general deficit in food consumption or taste preferences. Rather, *tmc* was selectively required to discriminate among foods with a broad range of hardness or viscosity.

To examine whether the deficit in food texture perception was due to the loss of *tmc*, we conducted genetic rescue experiments with the *tmc* cDNA. To clone the full-length cDNA from the proboscis, a primary taste organ analogous to the human tongue, we performed RT-PCR (Figure S2C). The *tmc* cDNA encoded a predicted protein of 1,932 amino acids, which was much larger than its counterparts in worms, mice and humans (757 to 1,285 amino acids) (Kurima et al., 2003). We found that the abnormality exhibited by *tmc¹* animals in sensing food hardness and viscosity was fully reversed by expressing the *tmc* cDNA (*UAS-tmc*) under control of the *tmc* promoter (*tmc-Gal4*; Figures 2C—2E and Figures S3A—S3C).

***tmc* localized to a previously unknown multidendritic neuron in the labellum**

To characterize the expression pattern of TMC, we generated TMC antibodies. As revealed by immunocytochemical assays, TMC was localized to a novel type of multi-dendritic neuron in the labellum (md-L) (Figure 3A). TMC was present in the dendritic terminals, implying a sensory role (Figure 3A). In contrast, we did not observe anti-TMC immunoreactivity in *tmc¹* animals, confirming the specificity of the TMC antibodies (Figure 3B). In order to acquire higher-resolution images of the processes of the md-L neuron, we generated a *tmc-Gal4* reporter transgene that included a 3 kb promoter region upstream of the *tmc* transcriptional start site. In combination with the *UAS-mCD8::GFP* reporter, we found that the *tmc-Gal4* specifically stained one multidendritic neuron in each of the two bilaterally symmetrical labella (Figure 3C). Based on double-labeling experiments with TMC antibodies, the neuron was identical to md-L (Figures S4A—S4C). The cell body of

the md-L neuron was positioned next to one of the I-type sensilla (I6) at the proximal part of the labella (Figure 3D). Remarkably, md-L neurons extended fine and elaborate dendritic branches innervating the bases of many sensilla, the majority of which (~70%) were L-type sensilla (Figure 3D). Other than md-L neurons, the *tmc-Gal4* reporter labeled a few multidendritic neurons in the ventral cibarial sensory organ (VCSO) (Figure 3E), an accessory taste organ analogous to the human pharynx. The multiple elaborate dendritic branches assembled into a brush-like structure that faced the luminal side of food-passing tunnel (Figure 3E), implying that they may sense the shearing force during food flow.

To examine the relative expression of md-L neurons and GRNs, we generated a *QF* line (Potter et al., 2010) using the same *tmc* promoter as for the *tmc-Gal4* line. We then performed double-labeling experiments with the *Gr5a-Gal4* reporter, which labels sugar-sensitive GRNs (Thorne et al., 2004; Wang et al., 2004). The *tmc* and *Gr5a* reporters labeled two morphologically different types of neurons in the labellum: the *tmc* reporter marked md-L neurons, while the *Gr5a* reporter stained bipolar GRNs (Figure 3F). The dendritic branches of md-L neurons entangled closely with the GRNs underneath the cuticle (Figure 3F). Furthermore, confocal imaging analysis revealed that many dendritic arbors of md-L neurons are closely associated with the cell bodies of GRNs (Figure 3G).

We also examined the projection pattern of the md-L axon in the central brain. The axonal terminals projected to subesophageal zone (SEZ) (Figure 3H), a brain region dedicated to processing taste input from the peripheral system. The particular region targeted by md-L neurons was different from that innervated by GRNs, such as those marked by the *Gr5a-Gal4* (Figure 3I). Other than the SEZ, the *tmc-Gal4* stained at least two other brain regions: ventral projection neurons of the antennal lobe and a subset of mushroom-body neurons (Figure 3H). We detected *tmc-Gal4* expression in a few neurons located at the wing hinge (Figure S4D) and the leg joint, indicating a potential role in proprioception (Figure S4E). However, we did not detect *tmc-Gal4* expression in the tarsal leg segment, a peripheral taste organ (Figure S4E). In summary, *tmc* molecularly defines a previously unrecognized sensory neuron in the fruit fly proboscis. The unique dendritic arborization pattern of md-L neurons at the bases of many sensilla suggests that these multidendritic neurons may detect compression forces arising from the bending of taste sensilla.

Activation of md-L neurons by mechanical deflection of taste sensilla

To investigate whether md-L neurons might be responsible for detecting mechanical stimuli applied to gustatory sensilla, we performed electrophysiological analysis. We deflected taste bristles using the tip of a fine glass pipet controlled by a piezoelectric activator system. Bending of taste sensilla produced stress at the base of sensilla, and may mechanically activate the underlying dendrites of md-L neurons. We identified the cell body of the md-L neuron using the I6 sensillum as a landmark. We also expressed a GFP reporter (*UAS-mCD8::GFP*) under control of the *tmc-Gal4*, and pinpointed the md-L cell body by fluorescent microscopy. We then recorded the electrophysiological responses of the md-L neuron with a recording electrode impaled in the vicinity of its cell body. This recording configuration allowed for single-unit recordings of md-L neuronal activity.

In *Drosophila*, sensory bristles extend from many body parts, such as the thorax, and exhibit planar cell polarity (Klein and Mlodzik, 2005). Similarly, most of the L-type taste bristles, which are associated with md-L dendrites, point from the dorsal side down to the ventral side. To determine if md-L neurons are sensitive to forces applied in a particular direction, we deflected wild-type L-type sensilla in four different directions: dorsal, ventral, anterior and posterior. Strikingly, when we bent the sensilla with a displacement of 20 μm in the dorsal direction, the md-L neurons fired rapidly adapting action potentials (Figures 4A and 4B; 8.0 ± 1.0 spikes/500 ms). In contrast, deflecting the sensilla in the ventral direction triggered 60% fewer spikes (Figures 4A and 4B; 3.2 ± 0.7 spikes/500 ms). When we bent the taste bristles the same distance in either the anterior or the posterior direction, the md-L neurons produced 25% of the spikes generated by a dorsal deflection (Figures 4A and 4B; spikes/500 ms: anterior, 2.0 ± 0.5 ; posterior, 1.8 ± 0.4). Furthermore, when we deflected the bristles in four directions over a range of distances (10–30 μm), the md-L neurons were still most sensitive to bending in the dorsal direction (Figures S5A—S5D). Taken together, these results demonstrated that md-L neurons were more sensitive to mechanical stimuli in the dorsal direction than any other direction.

Control of mechanosensory responses of md-L neurons by *tmc*

To determine whether the force-induced action potentials elicited by md-L neurons were dependent on *tmc*, we performed extracellular single-unit recordings. We found that there was a significant reduction in the mechanosensory responses of *tmc¹* flies regardless of the direction of sensilla deflection (Figures 4A and 4B; spikes/500 ms: dorsal, 1.3 ± 0.4 ; ventral, 0.5 ± 0.2 ; anterior, 0.4 ± 0.2 ; posterior, 0.3 ± 0.2). We rescued the electrophysiological defects by restoring expression of wild-type *tmc* (*UAS-tmc*) under control of the *tmc-Gal4* (Figures 4A and 4B; spikes/500 ms: dorsal: 8.5 ± 1.2 ; ventral: 3.5 ± 0.4 ; anterior: 2.2 ± 0.4 ; posterior: 2.1 ± 0.4). The dramatic reduction in force-induced action potentials in *tmc¹* was not due to a secondary consequence of a general impairment in labellar function since the mutant animals showed normal responses to salt, sucrose, and caffeine (Figures 4C—4E).

To explore further a requirement for md-L neurons and TMC for force-induced neuronal activity, we tested Ca^{2+} dynamics in the axonal terminals of md-L neurons in response to mechanical deflection. To visualize changes in Ca^{2+} levels in live animals, we expressed a transgene encoding the Ca^{2+} sensor GCaMP6f (*UAS-GCaMP6f*) (Chen et al., 2013) in md-L neurons under the control of the *tmc-Gal4*. We surgically exposed the SEZ region in the brain and monitored fluorescent changes as we pushed the taste sensilla toward the dorsal side with a polished glass probe. We found that mechanical stimuli led to robust Ca^{2+} influx in the axonal terminals of md-L neurons (Figures 5A, 5C and 5D). In contrast, no significant Ca^{2+} transients occurred in *tmc¹* mutant animals (Figures 5B—5D).

md-L neurons are required for food texture sensation

To provide additional evidence that md-L neurons were critical for discriminating foods based on texture, we performed cell-type-specific genetic manipulations. In addition to md-L, the *tmc-Gal4* was also expressed in a few central brain regions such as the mushroom bodies and the antennal lobes (Figure 3H). However, staining of these central brain regions may represent ectopic expression of the reporter since anti-TMC did not stain the mushroom

bodies and antennal lobes. Nevertheless, to test whether food texture sensation was solely mediated by md-L, we first performed intersectional genetic labeling using the *tmc-Gal4* line in combination with promoter-*Gal80* lines (Suster et al., 2004). We screened for promoter-*Gal80* lines that selectively repressed expression of the *tmc-Gal4* in the central brain. We successfully identified one *Gal80* line, *vGluT-Gal80* (Bussell et al., 2014), which specifically erased expression of the *tmc-Gal4* reporter in central brain regions, such as the mushroom bodies and antennal lobes, while leaving intact staining of the md-L projections into the SEZ (Figures 6A and 6B). In addition, given that the motor neurons controlling muscle movements in *Drosophila* are glutaminergic (Daniels et al., 2008), *vGluT-Gal80* serves to repress any potential *Gal4* mis-expression in motor neurons.

To test the requirement of md-L neurons for sensation of food mechanics, we used tetanus toxin (TNT) to shut down synaptic transmission between md-L and its synaptic partners. As we expected, *tmc-Gal4/UAS-TNT* animals exhibited a severe defect in sensing the hardness of agarose foods (0.5—4% agarose) (Figure 6C and Figures S6A and S6B), as well as the viscosity of HPC/sucrose solutions (0—1.5% HPC) (Figure 6C and Figure S6C). To determine if the behavioral abnormality was due to the md-L neurons, we combined the *vGluT-Gal80* transgene with the *tmc-Gal4* and *UAS-TNT* to abolish synaptic transmission exclusively in md-L neurons. We found that these animals showed the same extent of defects as *tmc-Gal4/UAS-TNT* animals (Figure 6C and Figures S6A—S6C). These results provide strong evidence that the single md-L neuron in each bilaterally symmetrical labellum governs the behavioral responses to food mechanics.

To reinforce the conclusion that the md-L neuron was indispensable for controlling food texture sensation, we used a laser (405 nm) to selectively compromise the md-L cell body. This neuron is positioned underneath a thin layer of cuticle on the surface of labellum, making laser treatments feasible (Figures 6D and 6E). We found that animals with ablated md-L somas displayed significant defects in sensing the hardness of solid food and the viscosity of liquid food (Figure 6F; Figures S6D and S6E). In summary, the intersectional genetic and laser treatment experiments demonstrate that md-L neurons play a critical role in orchestrating the sensation of food mechanics.

Optogenetic stimulation of md-L caused intensity-dependent effects on proboscis extension

To test if artificially activating md-L neurons in the proboscis is sufficient to produce behavioral responses, we employed a red-shifted channelrhodopsin, CsChrimson, to minimize behavioral artifacts caused by activation of the visual system (Klapoetke et al., 2014). We expressed *UAS-CsChrimson* under control of the *tmc-Gal4*. In addition to md-L, the *tmc-Gal4* was expressed only in a small number of local neurons in the adult ventral nerve cord (VNC), and projections extending from a few neurons in the legs or wing hinges (Figure S7A). To erase expression in the VNC, we employed a *Gal4* repressor that is expressed in VNC (*vGluT-Gal80*). Notably, this repressed almost all *tmc-Gal4* expression in the VNC (Figure S7B). To conduct the optogenetic analysis, we immobilized the animals' bodies within a small pipet tip, while allowing the proboscis to remain exposed and

unrestrained (Figure 7A). We then surgically removed the forelegs to exclude potential interference with the proboscis extension response (Figure 7A).

To gain a quantitative view of the correlation between md-L activation and motivation to feed, we monitored the PER assay, following stimulation of md-L neurons with red light (620 nm) of various intensities ranging from weak to strong (0.05 – 1 mW/mm²). Remarkably, we found that the animals immediately stretched their proboscises upon exposure to low or moderate levels of light (0.05–0.4 mW/mm²; Figure 7B and Movie S1). Once the light was turned off, the animal contracted its proboscis to the resting state (Figure 7C and Movie S1), indicative of a reversible behavioral process. Furthermore, to minimize potential light activation of *tmc* neurons in other parts of bodies such as the wing hinge and the leg joint, we shielded the fly body with aluminum foil (Figures 7D–7G). As with the preceding results, control animals displayed few PERs upon stimulation with either weak or strong light stimuli (Figures 7D, 7E, 7H and 7I). However, the *tmc-Gal4,UAS-CsChrimson* animal showed prominent PERs under weak light conditions (0.1 mW/mm²; Figures 7F, 7H and 7I). In contrast, under more intense light (0.6–1 mW/mm²), the PER was suppressed (Figures 7G, 7H and 7I). At the highest light intensity tested (1 mW/mm²), the animals contracted their proboscises (Movie S2). Thus, weak and moderate light promoted proboscis extension, which is associated with attraction to soft food, whereas strong light inhibited proboscis extension—a behavior associated with aversion to hard food.

To determine if the light-induced PER was due solely to activation of the md-L neuron, we subjected *tmc-Gal4,UAS-CsChrimson;vGlut-Gal80* animals to optogenetic analysis. We found that *tmc-Gal4,UAS-CsChrimson;vGlut-Gal80* animals showed proboscis extensions to weak light, as well as contraction of the proboscis by strong light, similar to the *tmc-Gal4,UAS-CsChrimson* animals (Figure 7I; Figures S8A and S8B). Controls expressing *UAS-CsChrimson* alone did not respond to light of either intensity (Figure 7I). Therefore, we conclude that the different levels of stimulation of md-L neurons lead to distinct behavioral outputs in the proboscis.

To test how the stimulation of md-L neurons with light of various intensities affect feeding, we presented a high concentration of sucrose solution (500 mM), while the animal was exposed to weak or strong light. Control animals that did not express *UAS-CsChrimson* showed similar PERs to 500 mM sucrose solutions regardless of light intensity (Figures 8A, 8B and 8E). In sharp contrast, as the light intensity rose, *tmc-Gal4,UAS-CsChrimson* animals showed a profound decline in the preference for the otherwise highly attractive sucrose (Figures 8C–8E), suggesting attraction to sucrose was significantly repressed by strong light. Similarly, *tmc-Gal4,UAS-CsChrimson;vGlut-Gal80* animals exhibited strong preferences for 500 mM sucrose under weak light (Figure 8F and Figure S8C), while they lost attraction to the same food under strong light (Figure 8F and Figure S8D). Taken together, stimulations of md-L neurons with varying light intensities differentially modulated sucrose feeding.

Discussion

We demonstrate that the attraction of wild-type flies to the same concentration of sucrose is altered by the viscosity or hardness of the food. If the sucrose-containing substrate is too sticky, soft or hard, the appeal of the food declines. These observations establish the *Drosophila* taste system as a model to explore the cellular and molecular underpinnings that allow an animal to sense food texture. Moreover, similar to the chemosensory evaluation of food by external sensilla decorating the labellum, the textural assessment of foods is also pre-ingestive in flies.

Requirement for md-L neurons for food texture sensation

We identified md-L—a previously undefined neuron in each of the two bilateral symmetrical labella, which extend a complex array of dendrites to the bases of many sensilla. Several observations demonstrate that md-L neurons play an indispensable role in food texture sensation. First, selective abolition of neurotransmission from md-L caused significant impairments in food texture discrimination. Second, laser ablation of md-L resulted in severe defects in perceiving the viscosity or hardness of foods. Third, low or moderate artificial activation of md-L neurons was sufficient to trigger proboscis extension. Thus, the loss-of-function and gain-of-function analyses of md-L neurons lead us to conclude that md-L neurons are key mechanoreceptor cells controlling sensation of food mechanics.

Unexpectedly, while low intensity optogenetic stimulation of md-L provoked proboscis extension, high intensity light induced contraction of the proboscis. Thus, md-L neurons are tuned to different levels of mechanical stimuli that give rise to drastically different feeding behaviors. We propose that weak or moderate light mimics the response to softer foods that simulates feeding, while strong light induces a higher level of activity that mimics hard foods and discourages feeding. When we offered a fly sucrose in combination with optogenetic stimulation of md-L neurons with strong light, this caused the animal to reject the otherwise appetitive food. We propose this rejection occurred because the animal perceived the texture of the sucrose as too hard. Thus, we suggest that texture sensation is mediated by md-L neuron through an intensity-dependent rather than a labeled-line mechanism. While md-L are required, we do not exclude that other neurons in the labella contribute to food texture sensation. Ultrastructural studies of taste sensilla led to the proposal that a neuron positioned at the base of each taste sensillum is a mechanosensory neuron (Falk et al., 1976). However, it currently remains unclear as to whether these neurons contribute to some aspect of food texture detection,

Directional sensitivity of md-L neurons

In *Drosophila*, most taste sensilla point toward the ventral direction. The md-L neuron produced much stronger neuronal activity in response to forces applied to taste hairs that were deflected dorsally than other directions. Thus, taste sensilla are most sensitive to force applied opposite to the direction in which they point. Notably, this direction-dependent feature of taste sensilla is reminiscent of the directional sensitivity of hair in mammals (Brown and Iggo, 1967; Gottschaldt and Vahle-Hinz, 1981; Lichtenstein et al., 1990;

Maruhashi et al., 1952; Rutlin et al., 2014), suggesting that it is a widely used neural coding strategy for sensation in the animal kingdom.

The directional sensitivity of taste sensilla differs from the macrochaete bristles in the thorax, since these latter bristles are most sensitive to force applied in the same direction in which they point (Walker et al., 2000). The profound differences in force directional sensitivity reflect the functional divergence between these two types of mechanosensory bristles. The direction-tuning feature of md-L neurons might be an evolutionary adaptation to help fruit flies sample food. While exploring the food landscape, a fruit fly normally extends its proboscis in the ventral direction. As a consequence, the forces arising from the food will bend taste sensilla in the opposite dorsal direction. Thus, we suggest that md-L neurons evolved to become most sensitive to forces emanating from the dorsal direction.

TMC is essential for food texture sensation

We conclude that *Drosophila* TMC is required for detecting food hardness. TMC is expressed and required in md-L neurons. Furthermore, loss of *tmc* greatly reduced the ability to behaviorally discriminate the preferred softness (1% agarose) or smoothness (sucrose solution only) from harder or stickier food options, respectively. However, the responses to tastants, such as sucrose, salt or caffeine, were unaffected in *tmc¹*, indicating that TMC was specifically required for sensing food texture rather than the chemical composition of food.

An important question concerns the mechanism through which TMC enables md-L neurons to sense food hardness. We propose that deflection of gustatory sensilla by food hardness imposes mechanical force on these neurons. The harder the food, the greater the stimulation of md-L neurons, which sense force through the dendrites innervating the bases of many sensilla. Given the expression of TMC in dendrites, an appealing possibility is that TMC is a key component of a mechanically-activated channel that endows the fly tongue with the ability to sense food hardness. A TMC protein (TMC-1) is expressed in worms and is proposed to be required for salt sensation (Chatzigeorgiou et al., 2013). Furthermore, TMC-1 plays a critical role in alkali sensation *in vivo* (Wang et al., 2016). As such, it appears that the worm TMC-1 controls multiple aspects of chemosensation. Two mammalian TMC1 and TMC2 are required for hearing and expressed in the inner ear (Kawashima et al., 2011; Pan et al., 2013). Currently, it is not known if mammalian TMCs are subunits of a channel, or whether they are mechanically activated, since problems with cell surface expression of these proteins in heterologous expression systems have precluded biophysical characterizations (Kawashima et al., 2011). In addition, TMCs may depend on additional subunits to form functional ion channels. Nevertheless, *Drosophila* TMC may be one subunit of a mechanically-activated channel, and we propose that this feature might allow md-L neurons to be stimulated in response to bending of taste sensilla by hard foods.

Conclusions and future perspective

In conclusion, we elucidated a cellular mechanism through which food mechanics influence the taste preference of an animal. The md-L neurons define a novel class of mechanosensory neurons that enable flies to detect food hardness and viscosity. A future question concerns

the mapping of the brain region where mechanical and chemosensory pathways converge to dictate gustatory decisions. An appealing possibility is that md-L and GRNs axons coordinately signal to a pair of command interneurons (Fdg neurons) that have extensive arborizations in the SEZ and control feeding behavior (Flood et al., 2013). Finally, our results demonstrate that TMC is essential for food texture sensation. These results raise the possibility that homologs of fly TMC may be dedicated to the gustatory discrimination of texture in many other animals including mammals.

Experimental Procedures

Control fly strains and outcrossing

The control flies were either *w¹¹¹⁸*, or Canton-S flies that were outcrossed to *w¹¹¹⁸*. All the mutants used were outcrossed to *w¹¹¹⁸* flies for five generations.

Null *tmc¹* mutant

To generate the *tmc¹* knock-out animals, we used ends-out homologous recombination (Gong and Golic, 2003) to create a 500 base pair deletion that removed the *tmc* genomic regions encompassing exons 14—16. This deletion eliminated 123 amino acid residues (1,133 to 1,255) encoding the TMC domain (Kurima et al., 2003) and altered the reading frame.

tmc transgenic lines

The *tmc-Gal4* and *tmc-QF* transgenes included a 3.0 kb genomic DNA fragment flanking the 5' end of the predicted transcriptional start site of *tmc*. The *UAS-tmc* transgene included a 5,799 bp *tmc* cDNA.

TMC antibodies

The TMC polyclonal antibodies were raised in rabbits in response to GST fused to a 72 amino acid C-terminal segment of TMC (residues 1,861—1,932).

Imaging immunostaining patterns

All immunostaining was performed using whole mounts of the indicated tissues and the images were acquired using a Zeiss LSM 700 confocal microscope.

Two-way choice feeding assays

To conduct the two-way choice assays, we used a Petri dish as previously described (Zhang et al., 2013). One half contained 2 mM sucrose and a particular concentration of agarose (0.5—5%), and the other half contained 2 mM sucrose and 1% agarose. The agarose foods were mixed with blue or red food dye. ~70 flies were starved for 24 hrs and allowed to choice between the two options for 90 minutes in the dark. We assessed the colors of the abdomens and calculated the preference index (PI). A PI=0 indicates no preference while PIs of 1.0 and -1.0 indicate complete preferences for one or the other food options. If the 1% agarose food was mixed with red dye, the $PI = (N_{red} + 0.5N_{purple}) - (N_{blue} + 0.5N_{purple}) / (N_{red} + N_{blue} +$

N_{purple}). If we mixed the blue dye with the 1% agarose, we calculated the PI as follows: $PI = (N_{\text{blue}} + 0.5N_{\text{purple}}) - (N_{\text{red}} + 0.5N_{\text{purple}}) / (N_{\text{red}} + N_{\text{blue}} + N_{\text{purple}})$.

Proboscis extension reflex (PER)

To perform the PER assays, we inserted a fly in a 200 μl pipet tip and touched the labellum with either a $\sim 2 \mu\text{l}$ drop of sucrose solution or to a small agarose ball formed at the end of pipet tip.

Mechanical response recordings

We immobilized flies by impaling them with a glass pipet. We deflected the sensilla 10–30 μm using a glass pipet mounted onto the tip of the piezoelectric actuator.

Tip recordings

We measured chemical-induced action potentials by performing tip recordings as described (Zhang et al., 2013a and 2013b). We used L4 or L6 sensilla to record the responses to HPC, NaCl, and sucrose, and S6 sensilla to record the responses to caffeine.

Ca²⁺ imaging

To perform the Ca²⁺ imaging in live animals, we expressed *UAS-GCaMP6f* (Chen et al., 2013) under the control of the *tmc-Gal4*. To determine the effect of force on Ca²⁺ dynamics, we applied force by pushing the labellum with a glass probe under the control of a piezoelectric system. To assess the responses to tastants, we applied a drop of liquid to the surface of the proboscis.

Laser treatments

We performed the laser treatments by placing the head of *tmc-Gal4/UAS-DsRed* flies in a pipet tip. We localized the md-L neuron using the red 568 nm laser line and directed a 405 nm laser line at nearly 100% power using a Zeiss LSM 700 confocal microscope.

Optogenetic assays

We performed optogenetic experiments using *tmc-Gal4/UAS-CsChrimson* flies that were prefed *all-trans*-retinal. We immobilized each animal in a pipet tip so that the proboscis was exposed to the outside, and stimulated the proboscis with red (620 nm, AmScope) or white light. In some experiments, the flies were offered a sucrose solution in the presence of varying intensities of light.

Statistical analysis

Unpaired Student's *t*-test was used to determine the statistical significance of two samples. To test the statistical significance of multiple samples, we used one-way ANOVA with Scheffé's post-hoc analysis.

See the Supplemental Experimental Procedures for further details.

Supplementary Material

Refer to Web version on PubMed Central for supplementary material.

Acknowledgments

We thank Christopher Potter, Loren L. Looger and the Bloomington Stock Center for providing fly stocks and reagents. We thank Bob Lansdorp and Omar Saleh at the Materials Department of UCSB, and Bruce Dunson at UCSB for assistance in setting up the piezoelectric system. We thank Jiangqu Liu for assistance with videotaping the proboscis extension reflex. This project was supported by a grant to CM from the National Institute on Deafness and other Communication Disorders (DC007864).

References

- Akitake B, Ren Q, Boiko N, Ni J, Sokabe T, Stockand JD, Eaton BA, Montell C. Coordination and fine motor control depend on *Drosophila* TRP γ . *Nat Commun.* 2015; 6:7288. [PubMed: 26028119]
- Benton R, Vannice KS, Gomez-Diaz C, Vosshall LB. Variant ionotropic glutamate receptors as chemosensory receptors in *Drosophila*. *Cell.* 2009; 136:149–162. [PubMed: 19135896]
- Brown AG, Iggo A. A quantitative study of cutaneous receptors and afferent fibres in the cat and rabbit. *J Physiol.* 1967; 193:707–733. [PubMed: 16992307]
- Bussell JJ, Yapici N, Zhang SX, Dickson BJ, Vosshall LB. *Abdominal-B* neurons control *Drosophila* virgin female receptivity. *Curr Biol.* 2014; 24:1584–1595. [PubMed: 24998527]
- Chatzigeorgiou M, Bang S, Hwang SW, Schafer WR. *tmc-1* encodes a sodium-sensitive channel required for salt chemosensation in *C. elegans*. *Nature.* 2013; 494:95–99. [PubMed: 23364694]
- Chen TW, Wardill TJ, Sun Y, Pulver SR, Renninger SL, Baohan A, Schreiter ER, Kerr RA, Orger MB, Jayaraman V, et al. Ultrasensitive fluorescent proteins for imaging neuronal activity. *Nature.* 2013; 499:295–300. [PubMed: 23868258]
- Daniels RW, Gelfand MV, Collins CA, DiAntonio A. Visualizing glutamatergic cell bodies and synapses in *Drosophila* larval and adult CNS. *J Comp Neurol.* 2008; 508:131–152. [PubMed: 18302156]
- Effertz T, Nadrowski B, Piepenbrock D, Albert JT, Göpfert MC. Direct gating and mechanical integrity of *Drosophila* auditory transducers require TRPN1. *Nat Neurosci.* 2012; 15:1198–1200. [PubMed: 22842145]
- Falk R, Bleiser-Avivi N, Atidia J. Labellar taste organs of *Drosophila melanogaster*. *J Morph.* 1976; 150:327–341.
- Flood TF, Iguchi S, Gorczyca M, White B, Ito K, Yoshihara M. A single pair of interneurons commands the *Drosophila* feeding motor program. *Nature.* 2013; 499:83–87. [PubMed: 23748445]
- Foster KD, Grigor JM, Cheong JN, Yoo MJ, Bronlund JE, Morgenstern MP. The role of oral processing in dynamic sensory perception. *J Food Sci.* 2011; 76:R49–61. [PubMed: 21535784]
- Freeman EG, Dahanukar A. Molecular neurobiology of *Drosophila* taste. *Curr Opin Neurobiol.* 2015; 34:140–148. [PubMed: 26102453]
- Galindo MM, Schneider NY, Stahler F, Tole J, Meyerhof W. Taste preferences. *Prog Mol Biol Transl Sci.* 2012; 108:383–426. [PubMed: 22656385]
- Gong WJ, Golic KG. Ends-out, or replacement, gene targeting in *Drosophila*. *Proc Natl Acad Sci USA.* 2003; 100:2556–2561. [PubMed: 12589026]
- Gottschaldt KM, Vahle-Hinz C. Merkel cell receptors: structure and transducer function. *Science.* 1981; 214:183–186. [PubMed: 7280690]
- Joseph RM, Carlson JR. *Drosophila* Chemoreceptors: A Molecular Interface Between the Chemical World and the Brain. *Trends Genet.* 2015; 31:683–695. [PubMed: 26477743]
- Kawashima Y, Geleoc GS, Kurima K, Labay V, Lelli A, Asai Y, Makishima T, Wu DK, Della Santina CC, Holt JR, et al. Mechanotransduction in mouse inner ear hair cells requires transmembrane channel-like genes. *J Clin Invest.* 2011; 121:4796–4809. [PubMed: 22105175]
- Keresztes G, Mutai H, Heller S. TMC and EVER genes belong to a larger novel family, the TMC gene family encoding transmembrane proteins. *BMC Genomics.* 2003; 4:24. [PubMed: 12812529]

- Kim SE, Coste B, Chadha A, Cook B, Patapoutian A. The role of *Drosophila* Piezo in mechanical nociception. *Nature*. 2012; 483:209–212. [PubMed: 22343891]
- Klapoetke NC, Murata Y, Kim SS, Pulver SR, Birdsey-Benson A, Cho YK, Morimoto TK, Chuong AS, Carpenter EJ, Tian Z, et al. Independent optical excitation of distinct neural populations. *Nat Methods*. 2014; 11:338–346. [PubMed: 24509633]
- Klein TJ, Mlodzik M. Planar cell polarization: an emerging model points in the right direction. *Annu Rev Cell Dev Biol*. 2005; 21:155–176. [PubMed: 16212491]
- Koc H, Vinyard CJ, Essick GK, Foegeding EA. Food oral processing: conversion of food structure to textural perception. *Annu Rev Food Sci Technol*. 2013; 4:237–266. [PubMed: 23244397]
- Koh TW, He Z, Gorur-Shandilya S, Menuz K, Larter NK, Stewart S, Carlson JR. The *Drosophila* IR20a clade of ionotropic receptors are candidate taste and pheromone receptors. *Neuron*. 2014; 83:850–865. [PubMed: 25123314]
- Kurima K, Peters LM, Yang Y, Riazuddin S, Ahmed ZM, Naz S, Arnaud D, Drury S, Mo J, Makishima T, et al. Dominant and recessive deafness caused by mutations of a novel gene, *TMC1*, required for cochlear hair-cell function. *Nat Genet*. 2002; 30:277–284. [PubMed: 11850618]
- Kurima K, Yang Y, Sorber K, Griffith AJ. Characterization of the transmembrane channel-like (TMC) gene family: functional clues from hearing loss and epidermodysplasia verruciformis. *Genomics*. 2003; 82:300–308. [PubMed: 12906855]
- Lichtenstein SH, Carvell GE, Simons DJ. Responses of rat trigeminal ganglion neurons to movements of vibrissae in different directions. *Somatosens Mot Res*. 1990; 7:47–65. [PubMed: 2330787]
- Liman ER, Zhang YV, Montell C. Peripheral coding of taste. *Neuron*. 2014; 81:984–1000. [PubMed: 24607224]
- Maruhashi J, Mizuguchi K, Tasaki I. Action currents in single afferent nerve fibres elicited by stimulation of the skin of the toad and the cat. *J Physiol*. 1952; 117:129–151. [PubMed: 14955805]
- Pan B, Geleoc GS, Asai Y, Horwitz GC, Kurima K, Ishikawa K, Kawashima Y, Griffith AJ, Holt JR. TMC1 and TMC2 are components of the mechanotransduction channel in hair cells of the mammalian inner ear. *Neuron*. 2013; 79:504–515. [PubMed: 23871232]
- Potter CJ, Tasic B, Russler EV, Liang L, Luo L. The Q system: a repressible binary system for transgene expression, lineage tracing, and mosaic analysis. *Cell*. 2010; 141:536–548. [PubMed: 20434990]
- Rolls ET. Taste, olfactory, and food texture processing in the brain, and the control of food intake. *Physiol Behav*. 2005; 85:45–56. [PubMed: 15924905]
- Rutlin M, Ho CY, Abaira VE, Cassidy C, Bai L, Woodbury CJ, Ginty DD. The cellular and molecular basis of direction selectivity of Adelta-LTMRs. *Cell*. 2014; 159:1640–1651. [PubMed: 25525881]
- Suster ML, Seugnet L, Bate M, Sokolowski MB. Refining GAL4-driven transgene expression in *Drosophila* with a GAL80 enhancer-trap. *Genesis*. 2004; 39:240–245. [PubMed: 15286996]
- Thorne N, Chromey C, Bray S, Amrein H. Taste perception and coding in *Drosophila*. *Curr Biol*. 2004; 14:1065–1079. [PubMed: 15202999]
- Vélez-Ruiz JF, Barbosa Cánovas GV. Rheological properties of selected dairy products. *Crit Rev Food Sci Nutr*. 1997; 37:311–359. [PubMed: 9227889]
- Vreugde S, Erven A, Kros CJ, Marcotti W, Fuchs H, Kurima K, Wilcox ER, Friedman TB, Griffith AJ, Balling R, et al. Beethoven, a mouse model for dominant, progressive hearing loss DFNA36. *Nat Genet*. 2002; 30:257–258. [PubMed: 11850623]
- Walker RG, Willingham AT, Zuker CS. A *Drosophila* mechanosensory transduction channel. *Science*. 2000; 287:2229–2234. [PubMed: 10744543]
- Wang X, Li G, Liu J, Liu J, Xu XZ. TMC-1 mediates alkaline sensation in *C. elegans* through nociceptive neurons. *Neuron*. 2016 in press.
- Wang Z, Singhvi A, Kong P, Scott K. Taste representations in the *Drosophila* brain. *Cell*. 2004; 117:981–991. [PubMed: 15210117]
- Westberg KG, Kolta A. The trigeminal circuits responsible for chewing. *Int Rev Neurobiol*. 2011; 97:77–98. [PubMed: 21708308]
- Whitehead MC, Beeman CS, Kinsella BA. Distribution of taste and general sensory nerve endings in fungiform papillae of the hamster. *Am J Anat*. 1985; 173:185–201. [PubMed: 20726120]

- Yan Z, Zhang W, He Y, Gorczyca D, Xiang Y, Cheng LE, Meltzer S, Jan LY, Jan YN. *Drosophila* NOMPC is a mechanotransduction channel subunit for gentle-touch sensation. *Nature*. 2013; 493:221–225. [PubMed: 23222543]
- Zhang YV, Raghuwanshi RP, Shen WL, Montell C. Food-experience induced taste desensitization modulated by the *Drosophila* TRPL channel. *Nat Neurosci*. 2013; 16:1468–1476. [PubMed: 24013593]

Author Manuscript

Author Manuscript

Author Manuscript

Author Manuscript

Highlights

- Fruit flies can discriminate foods based on hardness and viscosity.
- A force-activated multidendritic neuron (md-L) in the tongue senses food texture.
- Transmembrane channel-like (TMC) is critical for detecting food texture.
- Texture sensation by md-L neurons is mediated by an intensity coding mechanism.

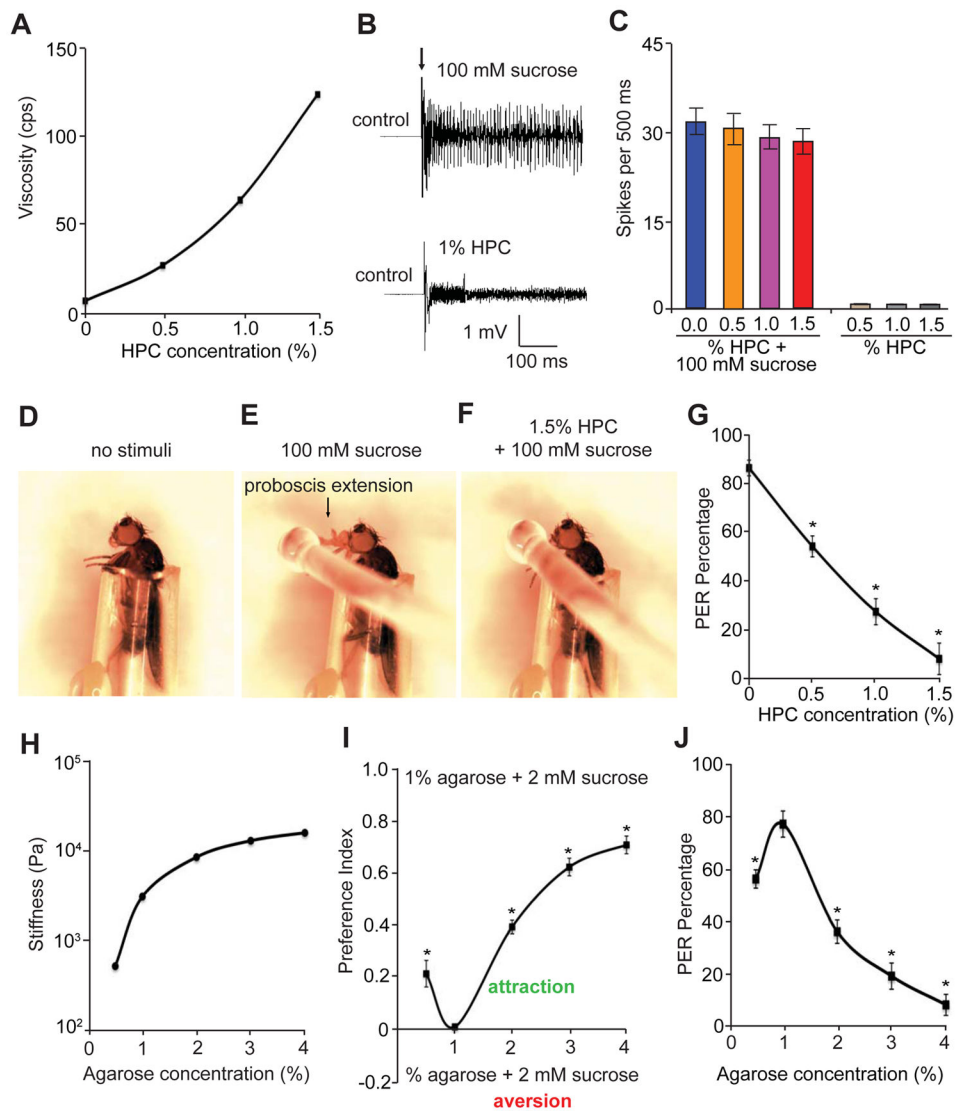


Figure 1. Feeding responses to liquid and solid foods with different viscosities and hardness, respectively

(A) Viscosities (centipoise) of solutions containing different concentrations of HPC (0—1.5%).

(B) Tip recordings of wild-type L4 sensilla showing the electrophysiological responses to either 100 mM sucrose or 1% hydroxypropyl cellulose (HPC).

(C) Average number of spikes produced in wild-type L4 sensilla in response to 0—1.5% HPC plus 100 mM sucrose or 0—1.5% HPC alone. $n=5$.

(D—F) Fly immobilized in a pipet tip for the proboscis extension reflex (PER) assay.

(D) Prior to presentation of a food stimulus to the fly.

(E) Fly stimulated with a drop of a 100 mM sucrose solution.

(F) Fly stimulated with a drop of a 1.5% HPC solution mixed with 100 mM sucrose.

(G) PER of control animals in response to stimulation with 0—1.5% HPC mixed with 100 mM sucrose. $n=20$.

(H) Rheological measurements of different percentages of agarose mixed with 2 mM sucrose. Stiffness was calculated by dividing the mechanical stress by the strain of the agarose gels. The stiffness unit is newton/meter² (pascal; Pa).

(I) Gustatory preferences exhibited by wild-type flies as a function of the agarose concentration. To perform the two-way feeding assays, one side of the Petri dish was filled with food made up of 1% agarose gel and 2 mM sucrose, and the other side contained 2 mM sucrose and agarose gels of varying percentages (0.5—4%) as indicated. ~70 adult flies/assay. n=5 trials.

(J) Percentages of the PER exhibited by control flies in response to stimulation with 0.5—4% agarose-containing food mixed with 100 mM sucrose. n=20. The error bars indicate SEMs. *p<0.05. ANOVA tests with Scheffé's post-hoc analysis.

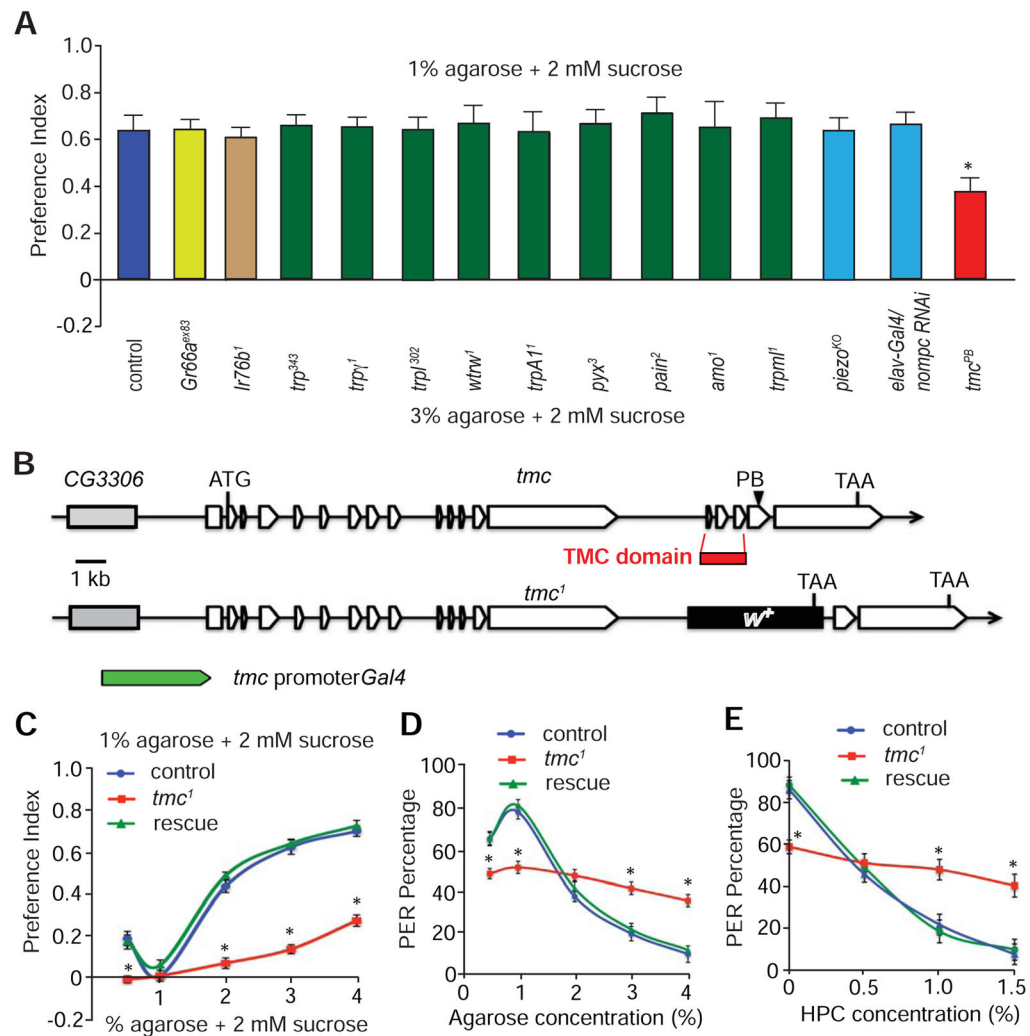


Figure 2. *tmc* mutant flies displayed impaired feeding responses to foods with different viscosity or hardness

(A) Screening of candidate receptors and channels for impacts on food selection based on hardness. The indicated animals were allowed to choose between 2 mM sucrose mixed with either 1% or 3% agarose using two-way food preference assays. The controls were *w¹¹¹⁸* flies. n=5 trials. ~70 flies for each trial.

(B) Genomic structures of the *tmc* gene and the strategy for making *tmc¹* knock-out flies by homologous recombination. The DNA fragment (red box) encoding the TMC domain was replaced by the *mini-white⁺* (*w⁺*) gene. To generate the *tmc* promoter *Gal4* line, we used the indicated 3 kb genomic DNA fragment flanking the 5' end of the transcriptional start site of *tmc*.

(C) Two-way feeding preferences exhibited by flies offered 1% agarose + 2 mM sucrose versus 2 mM sucrose containing various concentrations of agarose. The “rescue” flies in C—E are *tmc-Gal4/UAS-tmc;tmc¹*. n = 5 trials.

(D) The percentages of PER in response to stimulation with food containing 100 mM plus 0.5—4% agarose. n=20.

(E) The percentages of PER in response to presentation of 100 mM sucrose and 0—1.5% HPC. n=20.

The error bars indicate SEMs. *p<0.05. ANOVA tests with Scheffé's post-hoc analysis.

Author Manuscript

Author Manuscript

Author Manuscript

Author Manuscript

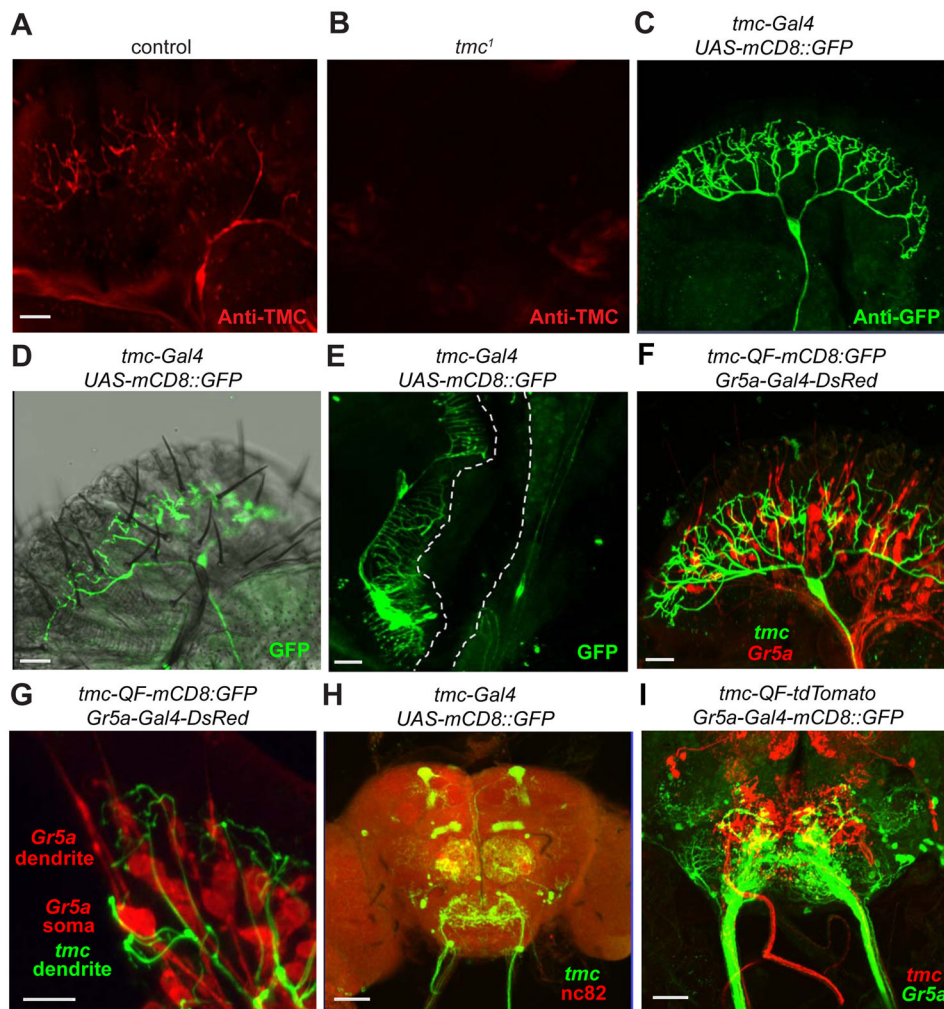


Figure 3. Expression pattern of *tmc* in the peripheral taste organ and the central brain

The staining patterns were viewed by confocal microscopy.

(A and B) Staining of labella using TMC antibodies.

(A) Control (*w¹¹¹⁸*).

(B) *tmc¹*.

(C) Anti-GFP staining of a labellum from flies expressing the *UAS-mCD8::GFP* reporter under control of the *tmc-Gal4*.

(D) The relative positions of md-L dendritic arbors (visualized by anti-GFP) and taste sensilla decorating the labella. Shown is a confocal image of anti-GFP staining superimposed on an image obtained by differential interference contrast. Representative S-, I- and L-type sensilla are marked. The I6 sensillum is indicated.

(E) Anti-GFP staining showing the expression pattern of the *tmc-Gal4* in the internal mouth.

(F) Double-labeling of *Gr5a* GRNs and md-L neurons in a labellum from *tmc-QF QUAS-mCD8::GFP; Gr5a-Gal4/ UAS-DsRed* flies. Green, anti-GFP; red, DsRed.

(G) A close-up view of the relative locations of md-L dendritic terminals (green), *Gr5a* GRN soma and dendrites (red) from *tmc-QF QUAS-mCD8::GFP; Gr5a-Gal4/ UAS-DsRed* flies.

(H) Central brain expression pattern of the *tmc-Gal4/UAS-mCD8::GFP* reporter. The axons of md-L neurons (green) project from the proboscis to the SEZ. Anti-nc82 (red) stains the active zones of neurons throughout the brain. AL, antennal lobe; MB, mushroom body; SEZ, subesophageal zone.

(I) Relative projection patterns of axons extending from *Gr5a* GRNs (green) and md-L neurons (red) into the SEZ of *tmc-QF QUAS-tdTomato;Gr5a-Gal4/UAS-mCD8::GFP* flies. The scale bars indicate 20 μm in all panels except for 10 μm in G and 40 μm in panel H.

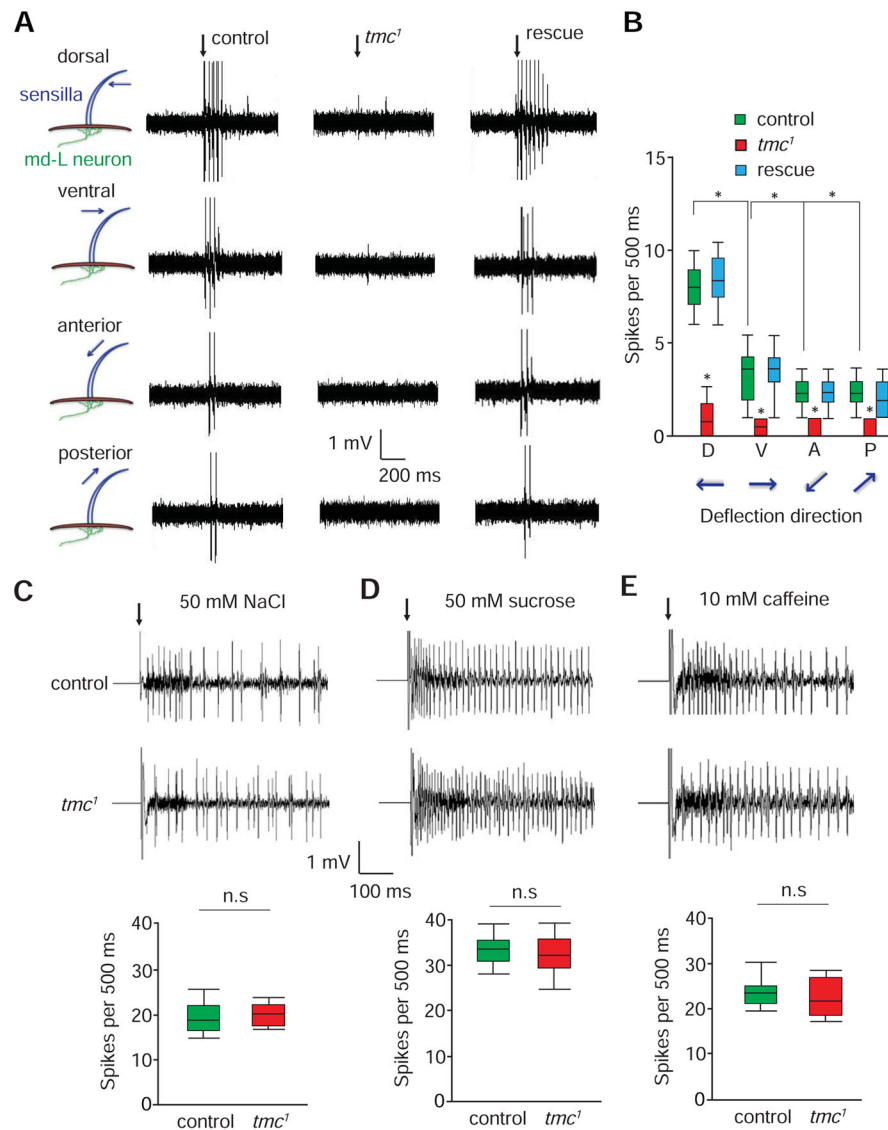


Figure 4. Electrophysiological responses of md-L neurons to mechanical stimuli

(A) Bending of L-type taste bristles exerted compression forces underneath dendritic arbors of md-L neurons, thereby leading to the firing of action potentials in md-L neurons. L4 taste bristles from the indicated flies were deflected 20 μ m in the dorsal, ventral, anterior and posterior directions. The rescue flies were *tmc-Gal4/UAS-tmc;tmc¹*. The vertical arrows indicate the onset of the mechanical stimuli.

(B) Box and whisker plots showing the number of spikes/500 ms. n=10.

(C–E) Tip recording traces showing the responses of control and *tmc¹* GRNs to chemical stimulation. The box and whisker plots show the summary tip recording data. Not significant, n.s. n=5.

(C) 50 mM NaCl (L4 sensilla).

(D) 50 mM sucrose (L4 sensilla).

(E) 10 mM caffeine (S6 sensilla).

The error bars indicate SEMs. * $p < 0.05$. ANOVA tests with Scheffé's post-hoc analysis.

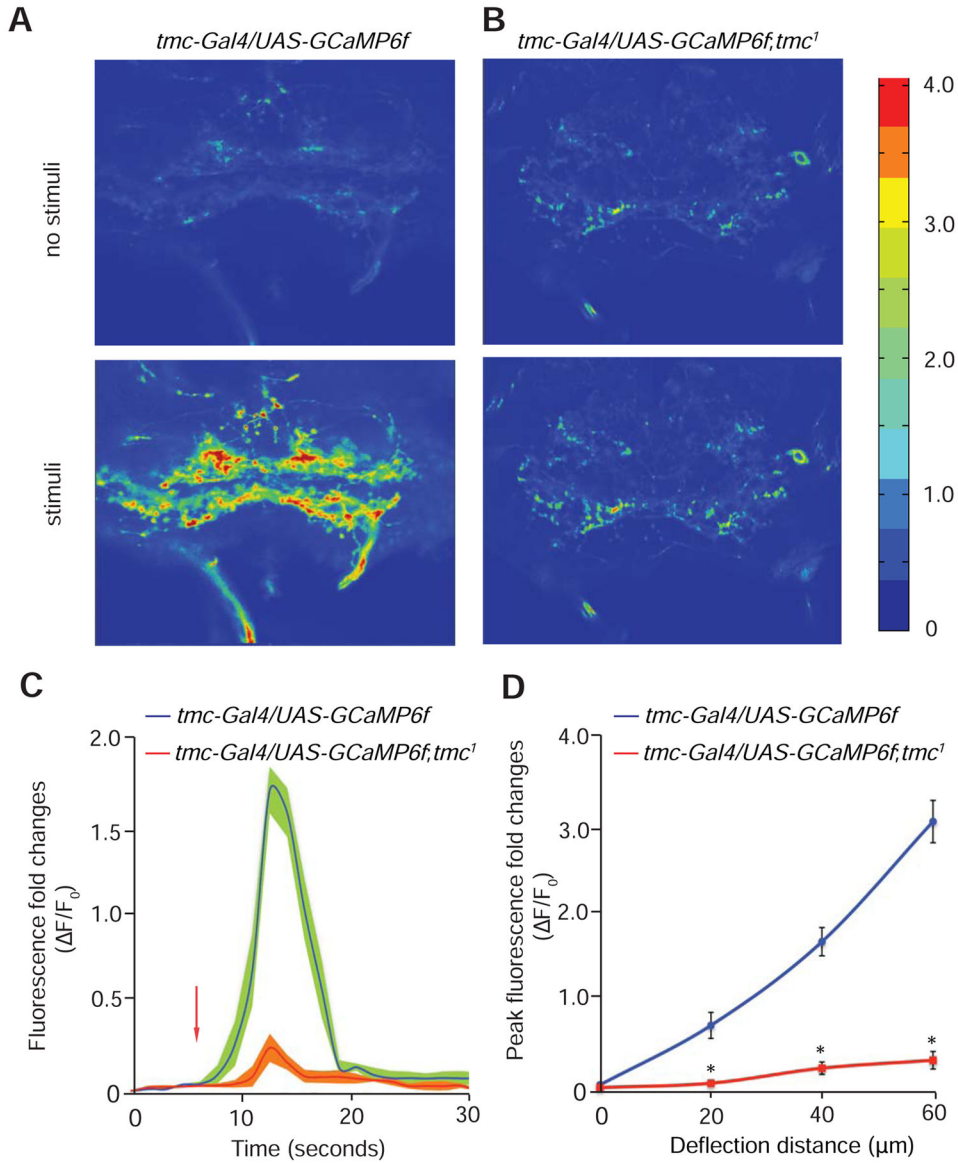


Figure 5. Ca²⁺ dynamics of *tmc* neurons in response to mechanical stimuli

(A and B) Representative images showing the relative changes in Ca²⁺ levels in the SEZ with and without mechanical stimulation of the labellum. The Ca²⁺ dynamics were monitored using GCaMP6f. The color scale to the right of (H) shows $\Delta F/F_0$.

(A) *tmc-Gal4,UAS-GCaMP6f*.

(B) *tmc-Gal4,UAS-GCaMP6f;tmc¹*.

(C) The time course showing the Ca²⁺ dynamics in the SEZ of *tmc-Gal4,UAS-GCaMP6f* and *tmc-Gal4,UAS-GCaMP6f;tmc¹* flies. Shown are the fold changes in fluorescence intensity ($\Delta F/F_0$). The arrow indicates the onset of mechanical stimuli. n=5.

(D) The fold changes in peak fluorescence intensity ($\Delta F/F_0$) in response to different deflection distances for *tmc-Gal4,UAS-GCaMP6f* and *tmc-Gal4,UAS-GCaMP6f;tmc¹* flies. n=5.

The error bars indicate SEMs. *p<0.01. ANOVA tests with Scheffé’s post-hoc analysis.

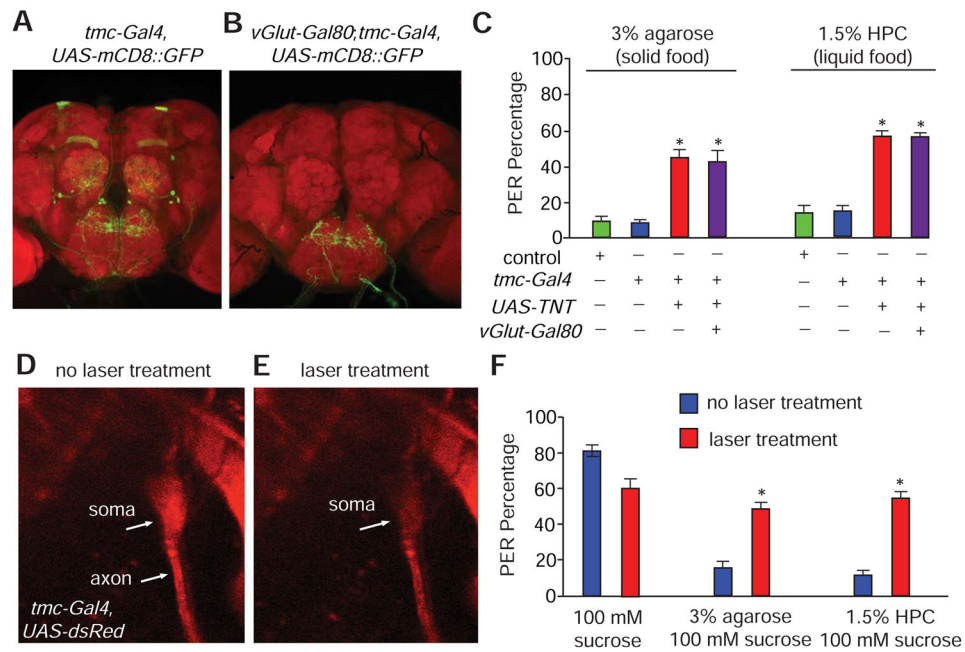


Figure 6. Requirements for md-L neurons for sensing food hardness and viscosity

(A and B) Intersectional genetic labeling of the central projections of md-L neurons.

(A) Central brain expression pattern of *tmc-Gal4,UAS-mCD8::GFP*.

(B) Central brain expression pattern of *tmc-Gal4,UAS-mCD8::GFP;vGluT-Gal80*.

(C) PER responses to foods containing 100 mM sucrose plus either 3% agarose or 1.5% HPC. Shown are the responses of controls and flies expressing the indicated transgenes. n=20.

(D and E) Images showing the soma and axon of an md-L neuron (*tmc-Gal4,UAS-DsRed*).

(D) Prior to laser treatment.

(E) After laser treatment.

(F) PER responses to foods containing 100 mM sucrose and either 3% agarose or 1.5% HPC before and after md-L neurons were exposed to laser treatments. n=15.

The error bars indicate SEMs. *p<0.05. ANOVA tests with Scheffé's post-hoc analysis.

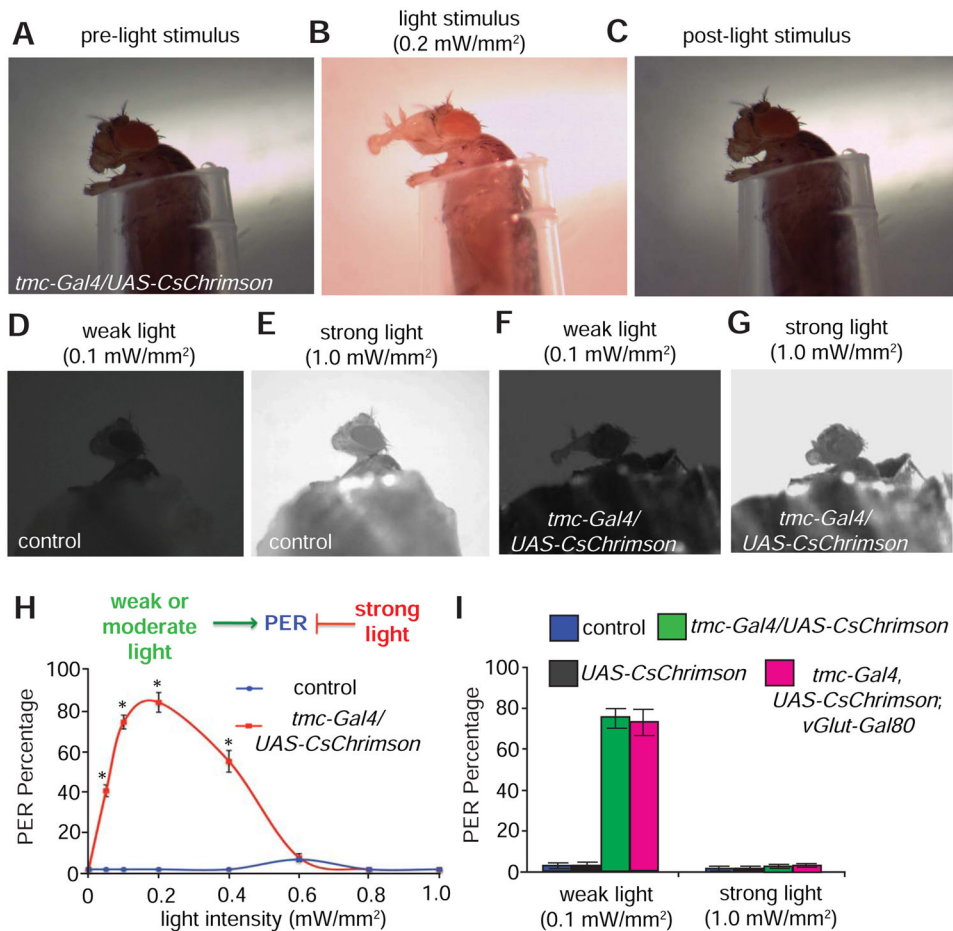


Figure 7. Optogenetic activation of md-L neurons is sufficient to trigger proboscis responses (A–C) Dynamics of light-induced proboscis extension in a fly expressing *tmc-Gal4,UAS-CsChrimson*.

(A) Prior to light stimulus.

(B) Full proboscis extension triggered by a moderate level of light (0.4 mW/mm²)

(C) Post-light stimuli.

(D) Lack of proboscis extension response upon exposure of control flies to weak light (0.1 mW/mm²).

(E) Lack of proboscis extension response upon exposure of control flies to strong light (1.0 mW/mm²).

(F) *tmc-Gal4/UAS-CsChrimson* flies extend their proboscis in response to weak light (0.1 mW/mm²).

(G) *tmc-Gal4/UAS-CsChrimson* flies retract their proboscis in response to strong light (1.0 mW/mm²).

(H) Relationship between the intensity of the stimulating light and percentages of the PER using the indicated flies. n = 15.

(I) Percentages of flies of the indicated genotypes showing PERs in response to weak (0.1 mW/mm²) or strong light stimuli (1 mW/mm²). n = 15.

The error bars indicate SEMs. *p<0.01. ANOVA tests with Scheffé's post-hoc analysis.

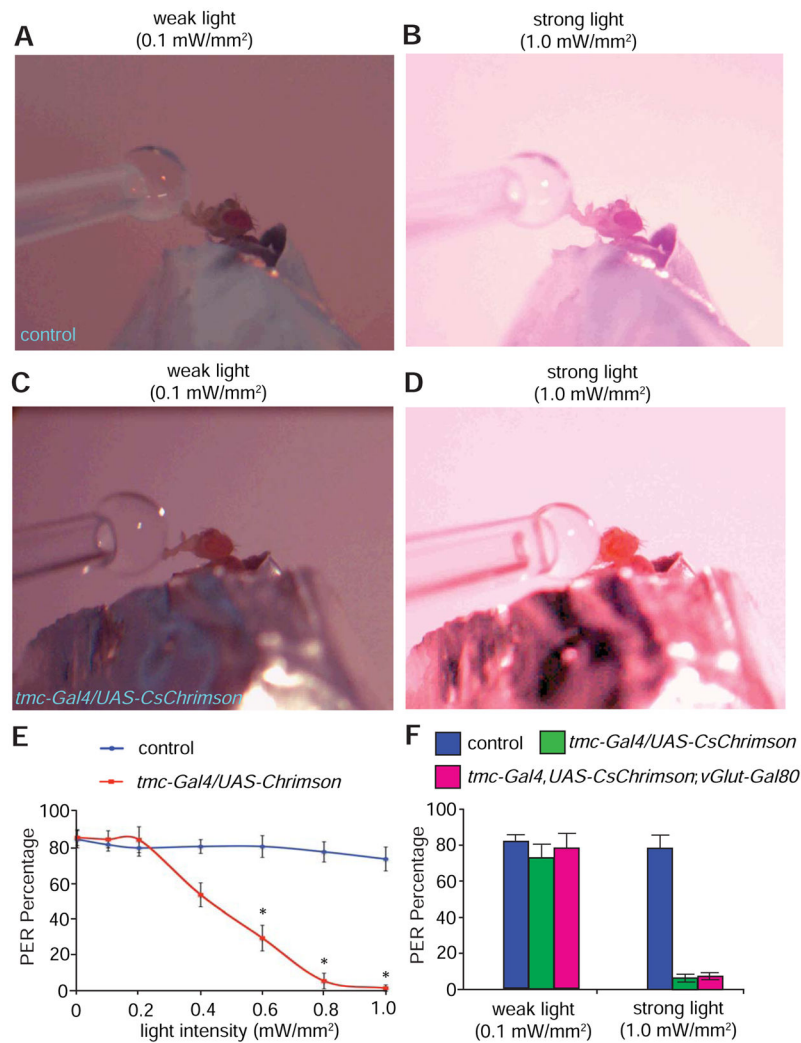


Figure 8. Differential modulation of sucrose feeding with varying intensities of light (A and B) PERs displayed by a control fly presented with 500 mM sucrose solution under: (A) weak light stimulation (0.1 mW/mm²), and (B) strong light stimulation (1.0 mW/mm²). (C) PER exhibited by a fly expressing *tmc-Gal4, UAS-CsChrimson* presented with 500 mM sucrose solution under weak light stimulation (0.1 mW/mm²). (D) No or minimal PER elicited by a fly expressing *tmc-Gal4, UAS-CsChrimson* presented with 500 mM sucrose solution under strong light stimulation (1.0 mW/mm²). (E) Relationship between the intensity of the stimulating light and PER percentages using the indicated flies. n = 15. (F) Percentages of flies of the indicated genotypes showing PERs in response to weak (0.1 mW/mm²) or strong light stimuli (1 mW/mm²). n = 15. The error bars indicate SEMs. *p<0.05. ANOVA tests with Scheffé's post-hoc analysis.